Taylor & Francis
Taylor & Francis Group

Inhalation Toxicology

International Forum for Respiratory Research

ISSN: 0895-8378 (Print) 1091-7691 (Online) Journal homepage: http://www.tandfonline.com/loi/iiht20

Forsterite exposure causes less oxidative DNA damage and lung injury than chrysotile exposure in rats

Ayako Takata, Hiroshi Yamauchi, Tadao Toya, Masahito Aminaka, Yasushi Shinohara, Norihiko Kohyama & Katsumi Yoshida

To cite this article: Ayako Takata, Hiroshi Yamauchi, Tadao Toya, Masahito Aminaka, Yasushi Shinohara, Norihiko Kohyama & Katsumi Yoshida (2009) Forsterite exposure causes less oxidative DNA damage and lung injury than chrysotile exposure in rats, Inhalation Toxicology, 21:9, 739-746, DOI: 10.1080/08958370802492399

To link to this article: https://doi.org/10.1080/08958370802492399

Inhalation Toxicology, 2009; 21(9): 739–746

informa
healthcare

ORIGINAL ARTICLE

Forsterite exposure causes less oxidative DNA damage and lung injury than chrysotile exposure in rats

Ayako Takata[1], Hiroshi Yamauchi[2], Tadao Toya[3], Masahito Aminaka[1], Yasushi Shinohara[3], Norihiko Kohyama[4], and Katsumi Yoshida[1]

[1]Department of Preventive Medicine, St. Marianna University School of Medicine, Kawasaki, [2]Department of Public Health, School of Allied Health Science, Kitasato University, Sagamihara, [3]National Institute of Occupational Safety and Health, Kawasaki, and [4]Natural Science Laboratory, Faculty of Economics, Toyo University, Tokyo, Japan

Abstract

Chrysotile (CH) is a pathogenic waste building material that can potentially be rendered innocuous via conversion to forsterite (FO) by heating at high temperatures. We compared the ability of FO and CH to cause oxidative DNA damage and lung injury. A single 1-mg intratracheal dose of CH or FO was administered to rats. Significant changes were observed 3 to 7 days after CH injection in alveolar macrophages, neutrophils, eosinophils, lymphocytes, total protein, and lactate dehydrogenase. High concentrations of 8-hydroxy-2′-deoxyguanosine (8-OHdG) were also observed in the macrophages, other infiltrating inflammatory cells, granulomas, and in bronchiolar and alveolar epithelial cells. The overexpression of 8-OHdG was limited to airway epithelial and inflammatory cells surrounding the fibrotic foci 540 days after injection, indicating that the inflammatory effects of CH were persistent yet decreased with time. Compared to the CH group, acute lung inflammation observed in the FO group was less apparent and exhibited no progressive fibrosing lesions. The expression of 8-OHdG was transient and weak in the bronchiolar epithelial cells as well as in the inflammatory cells, consistent with low concentrations of 8-OHdG observed in the lungs. These findings confirm that FO causes significantly less inflammation and oxidative DNA damage in the lungs than CH.

Keywords: *Chrysotile; synthetic forsterite; lung injury; oxidative DNA damage; 8-OHdG*

Introduction

Asbestos exposure causes asbestosis, lung cancer, mesothelioma, and pleural disease. Chrysotile (CH; $Mg_3Si_2O_5(OH)_4$) is the most commonly used form of asbestos in Japan. Based on current estimates, more than 1 million tons of debris containing CH will be generated every year for the next 20 yr by the demolition of condemned buildings. These staggering numbers have prompted discussion on the need to convert asbestos-containing wastes into harmless, recyclable materials.

One potential strategy capitalizes on the fact that CH exhibits dehydroxylation at approximately 550–700°C, followed by recrystallization to form forsterite (FO; Mg_2SiO_4) at approximately 700–800°C (Koshi et al., 1969; Hodgson, 1979; de Souza Santos & Yada, 1979). When it is further heated at 1000°C to 1200°C, a portion of the FO is converted into enstatite ($MgSiO_3$) (Koshi et al., 1969; Hodgson, 1979; de Souza Santos & Yada, 1979). Pilot testing has indicated that FO synthesized by heating CH at 1000°C can provide both refractoriness and reinforcement to materials, and it is thus a potentially attractive candidate for an alternative to asbestos in refractory products.

A limited number of studies have examined the biological effects of FO. Cytotoxicity studies in vitro have reported that FO is less toxic than CH (Koshi et al., 1969; Hayashi, 1974; Le Bouffant et al., 1983). Results obtained in vivo, however, are complicated. Woźniak et al. (1991) reported that rats that received intratracheal administration of FO exhibited greater increases in lung tissue concentrations of hydroxyproline, a biomarker for fibrosis, compared to rats that received CH 3 mo after injection. In contrast, another study reported that intrapleural administration of these materials to rats did not cause pleural neoplasm (Le Bouffant et al., 1983). However, when the material produced by heating CH at 850°C was intraperitoneally administered to rats, it caused peritoneal

Address for Correspondence: Ayako Takata, MD, PhD, 2-16-1 Sugao, Miyamae-ku, Kawasaki 216-8511, Japan, and Department of Preventive Medicine, St. Marianna University School of Medicine. E-mail: ayakot@marianna-u.ac.jp

(Received 21 July 2008; revised 21 September 2008; accepted 21 September 2008)

ISSN 0895-8378 print/ISSN 1091-7691 online © 2009 Informa UK Ltd
DOI: 10.1080/08958370802492399

mesothelioma with an incidence rate of 41% (Bolton et al., 1982). In sum, there are insufficient data on the toxicity and carcinogenicity of FO synthesized from CH.

Although the mechanism by which asbestos exposure causes oxidative DNA damage has not been clarified, there are two likely scenarios (Kamp & Weitzman, 1999; Shukula et al., 2003). The first potential mechanism directly involves free radicals generated by the iron-catalyzed reaction of asbestos fibers (Weitzman & Graceffa, 1984; Faux et al., 1994). The second potential mechanism involves indirect effects mediated by the secondary recruitment of inflammatory cells such as macrophages and neutrophils, as well as impaired macrophage phagocytosis (Goodglick & Kane, 1986; Hansen & Mossman, 1987). The second mechanism potentially plays a greater role than the first in the production of reactive oxygen species from CH with low iron concentrations (Poser et al., 2004). Reactive oxygen and nitrogen species thus appear to be important in asbestos-induced disease pathogenesis, although the mechanisms by which CH exposure causes oxidative DNA damage will require further attention.

As indicated earlier, CH is the primary type of asbestos that will require processing in Japan. We therefore compared biological effects of CH to those of FO generated by processing at 1000°C, as this is currently the most likely candidate end product. Intratracheal administration is a simple and effective method for comparative studies of respiratory toxicity, although the effects differ depending on the size or dosage of the fibers administered (Driscoll et al., 2000). A single intratracheal dose of CH or FO was administered to two groups of rats, and oxidative DNA damage and pathological and biochemical changes in lung tissue were subsequently monitored. Recently, 8-hydroxy-2′-deoxyguanosine (8-OHdG) has gained acceptance as a biomarker for oxidative DNA damage (Kasai & Nishimura, 1984; Kasai et al., 1986; Yamauchi et al., 2004; Kimura et al., 2006). For instance, significantly increased concentrations of 8-OHdG were observed in leukocyte DNA in workers exposed to asbestos (Takahashi et al., 1997; Marczynski et al., 2000a, 2000b) and in urine (Tagesson et al., 1993). We therefore utilized 8-OHdG to assess oxidative DNA damage.

Materials and methods

Materials

Fibers of less than 250 μm in length were separated from CH (grade AX) produced by Cassiar Mining Corp., British Columbia, Canada. This CH sample contained 2% Fe_2O_3 (ferric oxide) and 1% Al_2O_3 (aluminum oxide) as confirmed by x-ray fluorescence analysis. The instilled CH sample was analyzed for size distribution and numbers of fibers with an aspect ratio of 3 or greater and nonfibrous particles using a scanning electron microscope (SEM) (S4700; Hitachi High-Technologies Corporation, Tokyo). Table 1 summarizes the geometric mean length and diameter of fibers as well as the numbers of total particles and fibers in each length and diameter category.

Portions of the CH sample were heat-treated at 1000°C in an electric furnace for 1 h to synthesize FO. X-ray diffraction analysis revealed no residual CH. The FO sample contained a high level of enstatite (2:1 FO to enstatite ratio). X-ray fluorescence analysis revealed that the FO sample contained 2% Fe_2O_3 and 1% Al_2O_3, which was similar to corresponding concentrations in the CH sample. The long fibers in the CH sample were transformed into fine particles and fibrous particles, which are apparently seen as fibrous but consist of fine-grain aggregates in the FO sample (Figure 1). The number and size distribution of fibrous particles in the instilled FO sample analyzed by SEM are also summarized in Table 1.

Animal treatment

Each animal group consisted of five male Wistar rats (Clea Japan, Inc., Tokyo). Rats were housed in a barrier facility with a 12-h/12-h light–dark cycle, in which the room temperature and humidity were maintained at 24 ± 1°C and 55 ± 5%, respectively. There was a 2-wk acclimation period to the housing facility prior to experimentation.

CH or FO was administered to each rat at 10 wk of age. One group received only CH and another other group received only FO. Doses were prepared by suspending CH or FO in sterile saline solution using an ultrasonic cleaner (1 mg/0.5 ml). A single injection was administered intratracheally under halothane inhalation anesthesia. A third control group was administered 0.5 ml sterile saline solution using the same method. Rats were dissected under deep anesthesia induced by intraperitoneal administration of pentobarbital sodium on days 3, 7, 14, 30, 90, 180, 360, and 540. All procedures were approved by the Animal Research Committee at the National Institute of Occupational and Safety Health, Japan.

Analysis of bronchoalveolar lavage fluid (BALF)

Bronchoalveolar lavage fluid (BALF) analysis was performed between postinjection day 3 and day 90 to observe acute effects of CH and FO. BALF was collected using the method

Table 1. Number, length, and diameter distribution of instilled fibers in CH and FO samples.

	Number of fibers (× 10^6/mg)								Geometric mean length (μm)	Geometric mean diameter (μm)
		Length category (μm)			Diameter category (μm)					
Sample	Total fibers	<5	5–20	≥20	<0.1	0.1–0.5	0.5–1.0	≥1.0		
CH	5047 (96%) [a]	4124 (78%) [a]	843 (16%) [a]	79.1 (1.5%) [a]	1581 (30%) [a]	3439 (65%) [a]	26.4 (0.5%) [a]	0 (0%) [a]	2.00 (3.15) [b]	0.10 (1.57) [b]
FO	39.6 (50%) [a]	16.7 (42%) [a]	1.20 (7.2%) [a]	0.01 (0.5%) [a]	1.90 (2.4%) [a]	27.6 (35%) [a]	7.61 (10%) [a]	2.47 (3.1%) [a]	1.84 (2.30) [b]	0.30 (2.03) [b]

The number of total particles is 5271 × 10^6/mg in the CH sample and 79.5 × 10^6/mg in the FO sample.

[a] Percentage of fibers out of total particles.

[b] Geometric standard deviation.

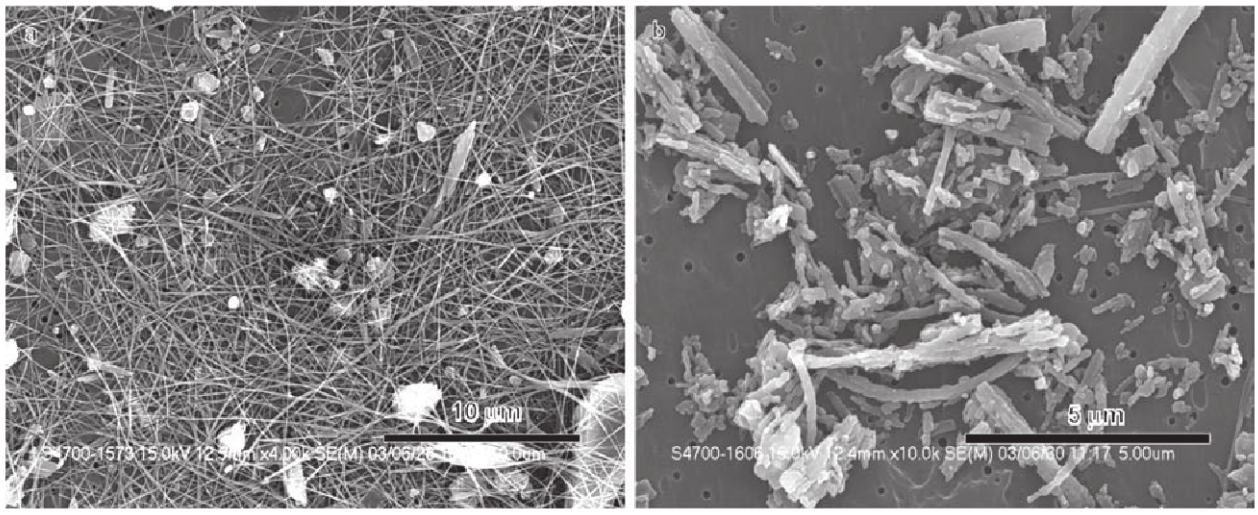

Figure 1. SEM images of CH and FO. (a) CH images. Magnification ×4,000. (b) FO images. Magnification ×10,000.

of Ishihara et al. (1999). Cell counts were performed on the BALF samples using an automatic hemocytometer (Sysmex F-800; Toa Medical Electronics Co., Ltd., Japan). Suspended cells in the BALF were centrifuged onto slides using a Cytospin 3 cytological centrifuge (Shandon, Switzerland). The slides were then stained with May–Grünwald–Giemsa. The numbers of cells greater than 500 were recorded for pulmonary alveolar macrophages (PAM), monocytes, neutrophils, eosinophils, and lymphocytes. Cell counts (cells/μl) for each inflammatory cell type were determined by multiplying the calculated percentage fraction of each cell type by the total number of cells.

The total protein (TP) and lactate dehydrogenase (LDH) in the supernatant of the BALF were measured biochemically. TP was determined using the Biuret method. LDH was measured using the tetrazolium salt method (lactate as substrate) using the Lactate dehydrogenase CII-test (Wako Pure Chemical Industries, Ltd., Osaka, Japan).

Histopathological examination

Tissue samples were perfusion fixed with phosphate-buffered 10% formalin. The lung and other major organ tissues were embedded in paraffin, sectioned, and then stained with hematoxylin-eosin (HE) and Masson's trichrome stain for collagen deposition. Pulmonary histopathology injury was classified using the scale described by Toya et al. (1999). Histopathological examinations in the lungs focused on the following features: alveolar macrophage recruitment, inflammation, granuloma, epithelial hyperplasia, interstitial fibrosis, and neoplasm. Histopathological features in the lungs were evaluated by scoring the distribution and severity of each lung lesion on a scale of 0 to 3, with grade 0 indicating "no changes or similar changes to those observed in the control group," grade 1 indicating "focal and mild changes," grade 2 indicating "moderate changes," and grade 3 indicating "marked changes."

Immunohistochemical staining for 8-OHdG

Immunohistochemical staining for 8-OHdG in the lungs was performed using the same paraffin blocks of lung tissues as used in the histopathological examinations. After deparaffinization, the sections were autoclaved at 120°C for 10 min for antigen retrieval. After quenching endogenous peroxidase activity, the sections were washed with phosphate-buffered saline (PBS), followed by skim milk for the reduction of nonspecific binding, and a final PBS wash. Anti-8-OHdG monoclonal antibody (MOG-020; Japan Institute for the Control of Aging, Shizuoka, Japan) was used as the primary antibody. After addition of anti-8-OHdG monoclonal antibody solution (dilution 1:100), the slides were incubated overnight at 4°C. The slides were then washed with PBS and incubated with biotin-labeled secondary antibody (Dako Japan Inc., Tokyo) at room temperature. After a further wash, the slides were treated with StreptAB complex/HRP (Dako Japan, Inc., Tokyo). The slides were washed again and treated with 3,3′-diaminobenzidine-tetrahydrochloride (Dako Japan, Inc., Tokyo) in order to visualize the reactions. The nuclei were counterstained with Meyer's hematoxylin.

HPLC–electrochemical detection (ECD) of 8-OHdG in lung tissue

Approximately 0.1 g of lung sample was homogenized in 3 ml ice-cold 0.15 *M* NaCl/0.1 *M* ethylenediamine tetraacetic acid (EDTA; pH 8.0) using a homogenizer (KINEMATICA, Switzerland). The nuclear fraction was collected via centrifugation at 1500 × *g* for 15 min at 4°C. This fraction was stirred with 1.5 ml 0.15 *M* NaCl/0.1 *M* EDTA (pH 8.0). After the subsequent addition of 2 ml lysis buffer (Applied Biosystems, USA) and 500 μl proteinase K (400 μg/ml; Wako Pure Chemical Industries, Ltd., Osaka, Japan), the reaction mixture was incubated at 50°C for 30 min. The reaction mixture was then mixed with 0.4 ml 2 *M* sodium acetate buffer (pH 4.5) and 8 ml ethanol, and DNA was collected using a Pasteur pipette. The DNA sample was cooled on ice and mixed with 100 μl of 100-U/ml nuclease P_1 (Wako Pure Chemical Industries, Ltd., Osaka, Japan) and 5 μl of 2 *M* sodium acetate buffer (pH 4.5) and then incubated at 37°C for 60 min. The DNA mixture was

then mixed with 80 μl of 1 *M* Tris-HCl buffer (pH 7.5) and 20 μl alkaline phosphatase (Sigma, USA), and incubated again at 37°C for 60 min. The sample was centrifuged at 10,000 × *g* for 3 min at 4°C, and the supernatant was collected and incubated at 50°C for 60 min. After the incubation, the supernatant was subjected to centrifugal filtration using 0.22-mm Ultrafree MC filters (Millipore, USA), followed by a further centrifugal filtration using Microcon centrifugal filter units (Millipore, USA).

8-OHdG in the filtered sample was analyzed using HPLC-ECD detection. Measurements were made using a Jasco Gulliver Series HPLC system (JASCO Corporation, Tokyo) equipped with a Coulochem II electrochemical detector (ESA, Inc., USA). At the same time, 2-deoxyguanosine (2-dG) was quantified using a UV detector. A reverse-phase partition column (Capcellpak C18 UG120, 4.6 × 250 mm; Shiseido, Tokyo) was used for HPLC. The column temperature and flow rate were 40°C and 0.8 ml/min, respectively. For the mobile phase, an 8% methanol/10 m*M* NaH_2PO_4 solution was used. Standard solutions of 8-OHdG (Wako Pure Chemical Industries, Ltd., Osaka, Japan) and 2-dG (Wako Pure Chemical Industries, Ltd., Osaka, Japan) were diluted to 5–20 ng/ml and 1–5 μg/ml, respectively. The level of 8-OHdG in the DNA was expressed as the number of residues per 10^6 guanine.

Statistical analysis

BALF analysis data and lung concentrations of 8-OHdG are summarized as mean ± standard deviation (SD). Data from the control group and the CH and FO groups, including BALF analysis results and lung concentrations of 8-OHdG, were subjected to one-way analysis of variance. Post hoc pairwise differences were assessed using Tukey's honestly-significant difference test (SPSS 15.0-J; SPSS Japan, Inc., Tokyo).

Results

BALF

Results of the BALF analysis are summarized in Table 2 until day 90 of the observation period. Cell counts and biochemical values did not change significantly during the entire observation period for the control group. For the CH group, cell counts on days 3 and 7 indicated a significant increase in neutrophil, eosinophil, and lymphocyte counts compared to controls ($p < .01$). Eosinophil and lymphocyte counts returned to normal levels after day 14, whereas neutrophils were significantly elevated until day 30. Likewise, the CH group exhibited a significantly higher increase in TP and LDH than did controls in the early observation period ($p < .01$), but was not significantly different from controls on day 30. In addition, injury

Table 2. Cell differentials and biochemical changes in rat BALF observed between day 3 and day 90.

		Days after intratracheal administration				
		3	7	14	30	90
BALF cells and differentials						
Total cells	Control	173 ± 11.5	200 ± 20.0	180 ± 34.6	180 ± 40.0	147 ± 11.5
(cells/μl)	CH	227 ± 23.1 **	167 ± 11.5	140 ± 20.0 #	133 ± 11.5	153 ± 30.6
	FO	200 ± 20.0 *	187 ± 41.6	220 ± 34.6	173 ± 23.1	173 ± 30.6
Macrophages	Control	172 ± 11.1	198 ± 19.5	179 ± 35.3	179 ± 40.3	145 ± 12.1
(cells/μl)	CH	91.0 ± 24.5 **, ##	107 ± 12.5 *, #	131 ± 19.6 #	131 ± 12.1	151 ± 30.4
	FO	187 ± 23.5	176 ± 38.5	217 ± 35.9	172 ± 22.9	172 ± 29.9
Monocytes	Control	0.07 ± 0.12	0.30 ± 0.15	0.20 ± 0.03	0.08 ± 0.13	0.36 ± 0.52
(cells/μl)	CH	7.47 ± 2.42 **, #	1.87 ± 0.38**, #	0.89 ± 0.23 *	0.25 ± 0.22	0.32 ± 0.28
	FO	2.77 ± 0.92	0.86 ± 0.04	0.90 ± 0.38	0.15 ± 0.13	0.26 ± 0.24
Neutrophils	Control	1.56 ± 1.59	0.87 ± 0.48	0.06 ± 0.10	0.27 ± 0.29	0.43 ± 0.27
(cells/μl)	CH	93.2 ± 11.1 ***, ###	22.1 ± 1.75 ***, ###	4.72 ± 1.61 **, #	1.94 ± 0.56 **, #	1.37 ± 0.74
	FO	5.55 ± 2.15	6.45 ± 2.33 *	1.73 ± 0.92	0.74 ± 0.23	0.78 ± 0.54
Eosinophils	Control	0.16 ± 0.27	0.16 ± 0.28	0.42 ± 0.54	0.01 ± 0.01	0.05 ± 0.08
(cells/μl)	CH	21.1 ± 5.91 **, ##	10.1 ± 3.77 **, ##	0.64 ± 0.10	0.05 ± 0.08	0.07 ± 0.12
	FO	3.22 ± 0.68	1.03 ± 0.50	0.23 ± 0.21	0.08 ± 0.14	0.01 ± 0.01
Lymphocytes	Control	0.01 ± 0.01	0.81 ± 0.13	0.47 ± 0.25	0.93 ± 0.71	0.41 ± 0.49
(cells/μl)	CH	13.9 ± 3.77 **, ##	25.7 ± 0.90 ***, ###	2.45 ± 1.39	0.50 ± 0.34	0.69 ± 0.46
	FO	1.97 ± 0.15	2.63 ± 1.40	0.55 ± 0.29	0.71 ± 0.23	0.53 ± 0.36
Biochemical parameters						
TP	Control	10.3 ± 1.53	9.67 ± 0.58	11.0 ± 0.45	11.0 ± 0.45	9.33 ± 1.53
(mg/dl)	CH	30.7 ± 9.07 **, #	16.0 ± 1.00 ***, ##	13.7 ± 0.58 *	11.7 ± 0.58	10.7 ± 0.58
	FO	14.3 ± 2.08	12.3 ± 0.58*	13.3 ± 1.16 *	12.0 ± 1.73	11.0 ± 0.45
LDH	Control	43.3 ± 11.0	44.0 ± 4.36	34.0 ± 1.73	38.3 ± 5.03	28.3 ± 2.89
(IU/L)	CH	137 ± 32.7 **, ##	72.0 ± 4.58 ***, ##	52.0 ± 6.08 *	36.0 ± 3.00	37.3 ± 6.81
	FO	61.7 ± 6.03	56.3 ± 2.08 *	47.3 ± 10.4	34.7 ± 3.51	37.7 ± 3.06

Note. Values are presented as mean ± SD. Significance indicated by:
*$p < .05$; **$p < .01$; ***$p < .001$ (compared to the control group);
#$p < .05$; ##$p < .01$; ###$p < .001$ (compared to the CH group).

to PAM was apparent for the early postadministration period and persisted throughout the observation period, delaying cell count recovery. In stark contrast, the FO group exhibited only a slight increase in neutrophil and eosinophil counts, and little or no injury to PAM was observed. Furthermore, TP and LDH were only slightly elevated for the FO group in the early observation period compared to controls.

Histopathology

Pulmonary lesions observed during the observational period are summarized in Table 3. No histopathological changes were observed from day 3 until day 540 in the control group, including inflammatory, granulomatous, and fibrotic lesions. Significantly more inflammatory responses were observed in the bronchioles, alveolar ducts, and alveoli on day 3 for the CH group compared to controls. Granulomas were identified in the bronchioles and alveolar ducts (Figure 2a). Bronchiolar epithelial hyperplasia and goblet-cell metaplasia were also apparent. Accumulation of alveolar macrophages was apparent and was observed multifocally in distal alveolar regions (Table 3).

Inflammatory responses gradually diminished after day 14 for the CH group. After day 30, collagen deposition within granulomas became more apparent in bronchioles and alveolar ducts. After day 90, fibrotic thickening of the alveolar walls was observed multifocally in distal alveolar regions as well (Table 3). This demonstrates that the reactions in alveolar regions were not caused by an agglomeration of fibers. Interstitial fibrosis was intense and extended to the bronchioles, alveolar ducts, and alveoli by day 540 (Figure 2b). Inflammatory cells infiltrated locally in the regions surrounding the granuloma and fibrotic lesions.

In contrast, lung lesions in the FO group were transient and considerably less severe than in the CH group. Inflammatory responses in the bronchioles, alveolar ducts, and alveoli were localized and mild on day 3. Furthermore, only a small number of microgranulomas were apparent in the peripheral airways (Figure 2c). Inflammatory responses had subsided by day 14. Neither the inflammatory responses nor the progressive fibrosing lesions detected in the CH group were apparent in the FO group on day 540 (Figure 2d). No neoplastic lesions were found in the CH and FO groups.

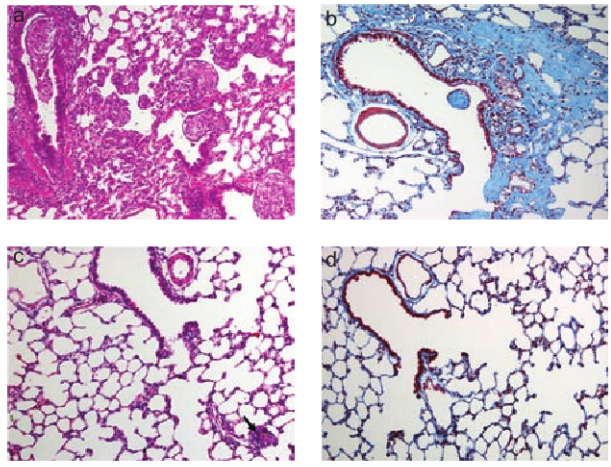

Figure 2. Lung histopathology. (a) CH day 3, hematoxylin and eosin (H-E) stain, original magnification ×200. Bronchiolitis and alveolitis were apparent. Foreign-body granulomas were apparent in the bronchioles and alveolar ducts. (b) CH day 540, Masson's trichrome stain, original magnification ×200. Fibrotic lesions were apparent in the bronchioles and alveolar ducts, and extended into the surrounding alveoli. (c) FO day 3, H-E stain, original magnification ×200. Slight infiltration of inflammatory cells was observed in the regions surrounding the bronchioles and in the alveoli. Microgranulomas were also observed (arrow). (d) FO day 540, Masson's trichrome stain, original magnification ×200. Inflammation and microgranulomas were minimal, and no fibrotic or neoplastic lesions were apparent.

Table 3. Lung histopathology severity for day 3 to day 540.

	Days after intratracheal administration																
	Control	CH								FO							
	3–540	3	7	14	30	90	180	360	540	3	7	14	30	90	180	360	540
Bronchi and bronchioles																	
Inflammation	0	2	2	2–1	1	1	1	1	1	1	1	0–1	0–1	0	0	0	0
Granuloma	0	2–3	3	2	2	2–1	2–1	1	1	0	0	0	0	0	0	0	0
Fibrosis	0	0	0	1	1–2	2	2–3	3	3	0	0	0	0	0	0	0	0
Reactive epithelial hyperplasia	0	2	2	2	2	1	1	1	1	1–2	1–2	1	0–1	0	0	0	0
Alveolar ducts																	
Inflammation	0	2–3	2–3	2	2–1	1	1	1	1	0–1	0–1	0–1	0–1	0	0	0	0
Granuloma	0	3	3	2	2–1	2–1	1	1	1	0–1	0–1	0	0	0	0	0	0
Fibrosis	0	0	0	1	1–2	2	2–3	3	3	0	0	0	0	0	0	0	0
Alveoli																	
Accumulation of PAM	0	2	2	2	2	1	1	1	1	1	1	0–1	0–1	0–1	0–1	0–1	0–1
Inflammation	0	2–3	2–3	1	1	1	1	1	1	1	1	0–1	0–1	0–1	0–1	0–1	0–1
Granuloma	0	1	1–2	1–2	1–2	1	1	0	0	0	0	0	0	0	0	0	0
Fibrosis	0	0	0	0	0–1	1	2	2–3	2–3	0	0	0	0	0	0	0	0

Note. The severity of histological changes was scored as "mild," "moderate," and "marked" (grades 1–3, respectively). A score of "zero" indicates that the finding was not observed. PAM, alveolar macrophages.

Localization of 8-OHdG in the lung

No 8-OHdG overexpression was detected via immunostaining for the control group during the entire observation period (Figure 3a). In contrast, 8-OHdG expression in the CH group was apparent starting on day 3 in macrophages, inflammatory cells that had infiltrated into the bronchioles, alveolar ducts, and alveoli. Nuclei of inflammatory cells within granulomas were also positive for 8-OHdG. Expression of 8-OHdG was not restricted to inflammatory cells, but extended into bronchiolar and alveolar epithelial cells. Expression of 8-OHdG was more marked on days 7 and 14 (Figure 3b), and became locally intensified in bronchiolar and alveolar epithelial cells and inflammatory cells surrounding fibrotic lesions. This expression pattern persisted until day 540 (Figure 3, c and d).

The expression of 8-OHdG was considerably weaker in the FO group than in the CH group, and was transient. Localized, weak expression of 8-OHdG was apparent in bronchiolar epithelial and inflammatory cells between day 3 and day 90 (Figure 3e). Little or no expression was apparent in the alveolar area. Expression was not detected on day 540 (Figure 3f).

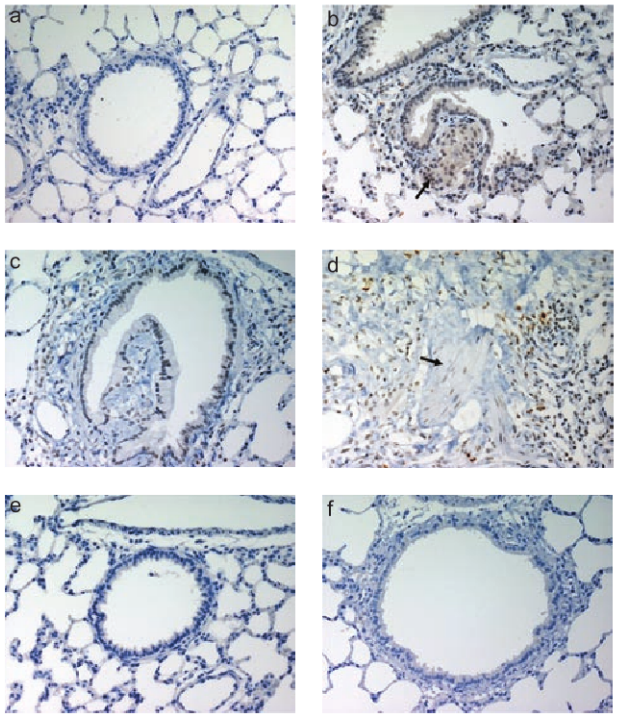

Figure 3. Immunohistochemical analysis of 8-OHdG in the lungs. Anti-8-OHdG monoclonal antibody was used for immunostaining. (a) Control day 14, original magnification ×400. No 8-OHdG expression was apparent in airway epithelial and inflammatory cells. (b) CH day 14, original magnification ×400. Nuclei of bronchiolar and alveolar epithelial cells as well as those of inflammatory cells (neutrophils, eosinophils, and macrophages) were positive for 8-OHdG. Nuclei of inflammatory cells within granulomas were also positive for 8-OHdG (arrow). (c) CH day 540, original magnification ×400. Nuclei of bronchiolar epithelial cells and interstitial inflammatory cells were positive for 8-OHdG. (d) CH day 540, original magnification ×400. Intense expression of 8-OHdG was apparent in the nuclei of alveolar epithelial cells and the inflammatory cells surrounding a fibrotic lesion (arrow). (e) FO day 14, original magnification ×400. No 8-OHdG expression was apparent in the airway epithelial and inflammatory cells. (f) FO day 540, original magnification ×400. No 8-OHdG expression was apparent in the airway epithelial and inflammatory cells.

Lung tissue 8-OHdG concentration

Changes in 8-OHdG concentration in lung tissue during the observation period are summarized in Figure 4. Concentrations were significantly higher for the CH group compared to controls for the entire period ($p < .001$), and the difference was most marked ($44.7 \pm 12.2/10^6$ dG) on day 14. Thereafter, lung concentrations of 8-OHdG decreased gradually. On day 540, lung 8-OHdG concentration was $11.7 \pm 1.95/10^6$dG for the CH group, which was approximately 5 times higher than the control value ($2.08 \pm 0.40/10^6$dG; $p < .001$). In contrast, differences between the FO group and controls were slight and not statistically significant for the entire observation period. Dynamics of lung 8-OHdG concentration were thus markedly different for the CH and FO groups.

Discussion

The biological effects of CH and FO synthesized from CH were assessed in vivo, with a focus on acute toxicity, lung fibrosis, and carcinogenicity. The effects of CH were generally consistent with previous findings (Wagner et al., 1974; Lemaire et al., 1985). Inflammatory responses were apparent in lung tissue soon after a single intratracheal administration of CH, and the results of BALF analysis (Table 2) were consistent with histopathological examination. Furthermore, immunostaining revealed localized expression of 8-OHdG in macrophages, infiltrating inflammatory cells, and granulomas starting 3 days after CH administration. This expression was not restricted to inflammatory cells, but extended to bronchiolar and alveolar epithelial cells. These observations are consistent with results of an examination of 8-OHdG concentrations made using the HPLC-ECD method (Figure 4). Notably, persistent expression of 8-OHdG was apparent 540 days after exposure using both instrumental analysis of 8-OHdG and immunostaining. This indicates that the deleterious effects of CH are highly sustained, and highlights the need for future evaluations of the biopersistence of CH in the lung and other tissues and organs.

Many factors likely determine the expression of 8-OHdG. The current results indicate that indirect effects mediated by

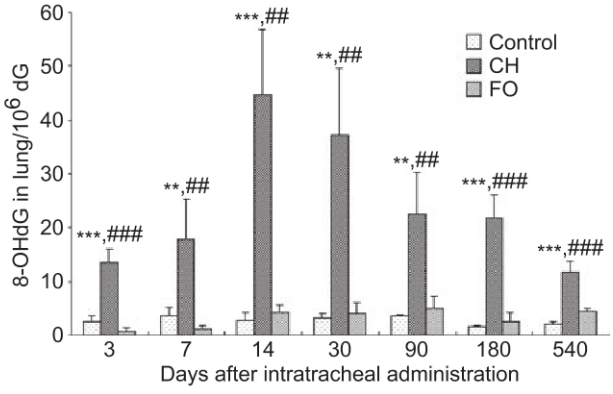

Figure 4. Time course of changes in lung 8-OHdG concentrations. Data are presented as mean ± SD. Significance indicated by $*p < .05$; $**p < .01$; $***p < .001$ (compared to the control group); $\#p < .05$; $\#\#p < .01$; $\#\#\#p < .001$ (compared to the CH group).

inflammatory cells such as macrophages and neutrophils are especially important. Fibers exceeding 20 μm in length that cannot be completely phagocytized by macrophages (Dörger et al., 2001) were included in the administered CH sample (Table 1). One possibility for the oxidative damage observed was that free radicals were overproduced in macrophages and inflammatory cells due to the long fibers included in the CH sample.

Previous observations are generally consistent with the present finding that CH induced inflammation and oxidative stress in fibrosis. Evidence obtained in vivo indicates that myeloperoxidase present in polymorphonuclear leukocytes, such as neutrophils, is involved in early oxidative stress following CH exposure (Haegens et al., 2005). Oxidative stress-induced heme oxygenase-1 (HO-1) expression has also been observed chronically in macrophages for up to six months after exposure (Nagatomo et al., 2007).

However, not all previous evidence is consistent with the current results. For instance, free radicals are involved in pulmonary inflammation and fibrosis for crocidolite with high iron content (Mossman et al., 1990; Ghio et al., 1998). Furthermore, administration of an iron chelator attenuated amosite-induced pulmonary inflammation and fibrosis in rats (Kamp et al., 1995). These findings suggest that asbestos with high iron content induces lung damage via oxidative stress promoted by an iron-catalyzed reaction. This mechanism is likely of little significance for damage due to CH, which contains minimal iron (2% Fe_2O_3). Indeed, one in vitro study demonstrated that an iron chelator could not prevent the generation of reactive oxygen species by CH with low iron content (Poser et al., 2004). However, another in vitro study indicated that metallic ions and fiber surface conditions are involved in CH-induced oxidative stress, in addition to fiber size (Gazzano et al., 2005). These varied results indicate that mechanisms for oxidative stress following CH exposure are complex and depend on many factors, including the specific composition of the CH.

All data obtained in the current study clearly indicate that the severity of acute inflammation and oxidative DNA injury in lung tissue was far less for FO compared to CH. Notably, FO did not induce the expression of 8-OHdG, as assessed via instrumental analysis and immunostaining. This indicates that FO did not cause oxidative DNA injury, suggesting that FO is less carcinogenic than CH. Indeed, previous animal studies have noted reduced carcinogenicity for FO compared to CH (Bolton et al., 1982; Le Bouffant et al., 1983). The current findings regarding FO are thus clearly important and have clear practical ramifications. However, it is important to highlight the fact that only a limited number of international studies have been conducted on FO. Thus, it is currently impossible to conclusively evaluate our results against an established body of literature.

It is possible that low FO toxicity resulted partially from the particular characteristics of the FO used in this study. The iron content of raw CH and synthetic FO was approximately 2%, and the biological effects of iron impurities were thus likely contained negligible amounts of both substances. However, fibrous particles of FO transformed from CH fibers are brittle because they consist of aggregated grains. The SEM analysis revealed that the number of fibers in the FO sample decreased significantly compared to that of the CH, and decreased even further when the fibers were longer and had a smaller diameter (Table 1). The number of fibers longer than 20 μm in the FO sample was about 1/1000th the number of fibers in the CH sample. Thus, differences in fiber size for FO compared to CH could have contributed to the differences in biological activity. Moreover, the fibrous morphology of FO particles can vary depending on the heat-processing temperature used for synthesis and on the method used for fiber pulverization. It is thus necessary to evaluate the biological effects of FO synthesized using a variety of techniques if practical solutions for the conversion of asbestos into inert materials are to be achieved.

In summary, we found that pathogenic effects of FO were far less than CH during a 540-day observation period in rats. These results indicate that one promising technique for curtailing the toxicity of asbestos and risk to humans is to convert it into FO via heat treatment. However, a great deal of future experimentation will be necessary to create practical solutions. In addition to determining heat conversion methods that optimally lead to reduced toxicity, it will be necessary to consider alternative processing methods that make fewer energy demands in order to limit the negative environmental impacts of asbestos abatement.

Declaration of interest

This study was endorsed and supported by the Agency of Natural Resources and Energy, Grant for mine/mineral exploration projects, and by the Japan Society for the Promotion of Science, Grant-in-Aid for Young Scientists (B) (number 15790289) and Grant-in-Aid for Scientific Research (C) (number 18590576). The authors alone are responsible for the content and writing of the paper.

References

Bolton, R. E., Davis, J. M. G., Donaldson, K., and Wright, A. 1982. Variations in the carcinogenicity of mineral fibres. *Ann. Occup. Hyg.* 26:569–582.

de Souza Santos,H. and Yada K. 1979. Thermal transformation of chrysotile studied by high resolution electron microscopy. *Clays Clay Miner.* 27:161–174.

Dörger, M., Münzing, S., Allmeling, A.M., Messmer, K., and Krombach, F. 2001. Differential responses of rat alveolar and peritoneal macrophages to man-made vitreous fibers in vitro. *Environ. Res.* 85:207–214.

Driscoll, K. E., Costa, D. L., Hatch, G., Henderson, R., Oberdorster, G., Salem, H., and Schlesinger, R. B. 2000. Intratracheal instillation as an exposure technique for the evaluation of respiratory tract toxicity: Uses and limitations. *Toxicol. Sci.* 55:24–35.

Faux, S. P., Howden, P. J., and Levy, L. S. 1994. Iron-dependent formation of 8-hydroxydeoxyguanosine in isolated DNA and mutagenicity in Salmonella typhimurium TA102 induced by crocidolite. *Carcinogenesis* 15:1749–1751.

Gazzano, E., Foresti, E., Lesci, I. G., Tomatis, M., Riganti, C., Fubini, B., Roveri, N., and Ghigo, D. 2005. Different cellular responses evoked by natural and stoichiometric synthetic chrysotile asbestos. *Toxicol. Appl. Pharmacol.* 206:356–364.

Ghio, A. J., Kadiiska, M. B., Xiang, Q. H., and Mason, R. P. 1998. In vivo evidence of free radical formation after asbestos instillation: an ESR spin trapping investigation. *Free Radical Biol. Med.* 24:11–17.

Goodglick, L. A., and Kane, A. B. 1986. Role of reactive oxygen metabolites in crocidolite asbestos toxicity to mouse macrophages. *Cancer Res.* 46:5558–5566.

Haegens, A., van der Vliet, A., Butnor, K. J., Heintz, N., Taatjes, D., Hemenway, D., Vacek, P., Freeman, B. A., Hazen, S. L., Brennan, M. L., and Mossman, B. T. 2005. Asbestos-induced lung inflammation and epithelial cell proliferation are altered in myeloperoxidase-null mice. *Cancer Res.* 65:9670–9677.

Hansen, K., and Mossman, B. T. 1987. Generation of superoxide ($O_2^-\bullet$) from alveolar macrophages exposed to asbestiform and nonfibrous particles. *Cancer Res.* 47:1681–1686.

Hayashi, H. 1974. Cytotoxicity of heated chrysotile. *Environ. Health Perspect.* 9:267–270.

Hodgson, A.A. 1979. Chemistry and physics of asbestos. *In Asbestos: Properties, applications and hazards,* eds. L. Michaels and S. S. Chissick, vol. 1, pp. 67–114. New York: John Wiley & Sons.

Ishihara, Y., Kyono, H., Kohyama, N., Otaki, N., Serita, F., Toya, T., and Kagawa, J. 1999. Acute biological effects of intratracheally instilled titanium dioxide whiskers compared with nonfibrous titanium dioxide and amosite in rats. *Inhal. Toxicol.* 11:131–149.

Kamp, D. W., Israbian, V. A., Yeldandi, A. V., Panos, R. J., Graceffa, P., and Weitzman, S. A. 1995. Phytic acid, an iron chelator, attenuates pulmonary inflammation and fibrosis in rats after intratracheal instillation of asbestos. *Toxicol. Pathol.* 23:689–695.

Kamp, D. W., and Weitzman, S. A. 1999. The molecular basis of asbestos induced lung injury. *Thorax* 54:638–652.

Kasai, H., and Nishimura, S. 1984. Hydroxylation of deoxyguanosine at the C-8 position by ascorbic acid and other reducing agents. *Nucleic Acids Res.* 12: 2137–2145.

Kasai, H., Crain, P. F., Kuchino, Y., Nishimura, S., Ootsuyama, A., and Tanooka, H. 1986. Formation of 8-hydroxydeoxyguanine moiety in cellular DNA by agents producing oxygen radicals and evidence for its repair. *Carcinogenesis* 7: 1849–1851.

Kimura, S., Yamauchi, H., Hibino, Y., Iwamoto, M., Sera, K., and Ogino, K. 2006. Evaluation of urinary 8-hydroxydeoxyguanine in healthy Japanese people. *Basic Clin. Pharmacol. Toxicol.* 98:496–502.

Koshi, K., Hayashi, H., and Sakabe, H. 1969. Biological and mineralogical studies on serpentine minerals in heat treated state. *Ind. Health* 7:66–85.

Le Bouffant L., Bruyère, S., Daniel, H., Martin, J.-C., Henin, J.-P., Tichoux, G., Nattier, P. 1983. Influence d'un traitement thermique des fibres de chrysotile sur leur comportement dans le poumon. *Pollution Atmosphérique* 97:44–49 (in French).

Lemaire, I., Nadeau, D., Dunnigan, J., and Massé, S. 1985. An assessment of the fibrogenic potential of very short 4T30 chrysotile by intratracheal instillation in rats. *Environ. Res.* 36:314–326.

Marczynski, B., Rozynek, P., Kraus, T., Schlösset, St., Raithel, H. J., and Baur, X. 2000a. Levels of 8-hydroxy-2'-deoxyguanoseine in DNA of white blood cells from workers highly exposed to asbestos in Germany. *Mutat. Res.* 468:195–202.

Marczynski, B., Kraus, T., Rozynek, P., Raithel, H. J., and Baur, X. 2000b. Association between 8-hydroxy-2'-deoxyguanoseine levels in DNA of workers highly exposed to asbestos and their clinical data, occupational and non-occupational confounding factors, and cancer. *Mutat. Res.* 468:203–212.

Mossman, B. T., Marsh, J. P., Sesko, A., Hill, S., Shatos, M. A., Doherty, J., Petruska, J., Adler, K. B., Hemenway, D., Mickey, R., Vacek, P., and Kagan, E. 1990. Inhibition of lung injury, inflammation, and interstitial pulmonary fibrosis by polyethylene glycol-conjugated catalase in a rapid inhalation model of asbestosis. *Am. Rev. Respir. Dis.* 141:1266–1271.

Nagatomo, H., Morimoto, Y., Ogami, A., Hirohashi, M., Oyabu, T., Kuroda, K., Higashi, T., and Tanaka, I. 2007. Change of heme oxygenase-1 expression in lung injury induced by chrysotile asbestos in vivo and in vitro. *Inhal. Toxicol.* 19:317–323.

Poser, I., Rahman, Q., Lohani, M., Yadav, S., Becker, H. H., Weiss, D. G., Schiffmann, D., and Dopp, E. 2004. Modulation of genotoxic effects in asbestos-exposed primary human mesothelial cells by radical scavengers, metal chelators and a glutathione precursor. *Mutat Res.* 559:19–27.

Shukula, A., Gulumian, M., Hei, T. K., Kamp, D., Rahman, Q., and Mossman, B. T. 2003. Multiple roles of oxidants in the pathogenesis of asbestos-induced diseases. *Free Radical Biol. Med.* 34:1117–1129.

Tagesson, C., Chabiuk, D., Axelson, O., Barański, B., Palus, J., and Wyszyńska, K. 1993. Increased urinary excretion of the oxidative DNA adduct, 8-hydroxydeoxyguanosine, as a possible early indicator of occupational cancer hazards in the asbestos, rubber, and azo-dye industries. *Pol. J. Occup. Med. Environ. Health* 6:357–368.

Takahashi, K., Pan, G., Kasai, H., Hanaoka, T., Feng, Y., Liu, N., Zhang, S., Xu, Z., Tsuda, T., Yamato, H., Higashi, T., and Okubo, T. 1997. Relationship between asbestos exposure and 8-hydroxydeoxyguanosine levels in leukocytic DNA of workers at a Chinese asbestos-material plant. *Int. J. Occup. Environ. Health* 3:111–119.

Toya, T., Fukuda, K., Kohyama, N., Kyono, H., and Arito, H. 1999. Hexavalent chromium responsible for lung lesions induced by intratracheal instillation of chromium fumes in rats. *Ind. Health* 37:36–46.

Wagner, J. C., Berry, G., Skidmore, J. W., and Timbrell, V. 1974. The effects of the inhalation of asbestos in rats. *Br. J. Cancer* 29:252–269.

Weitzman, S. A., and Graceffa, P. 1984. Asbestos catalyzes hydroxyl and superoxide radical generation from hydrogen peroxide. *Arch. Biochem. Biophys.* 228:373–376.

Woźniak, H., Więcek, E., and Bienlichowska-Cybula, G. 1991. The fibrogenic activity and neurotoxicity of heat-treated chrysotile. *Pol. J. Occup. Med. Environ. Health* 4:21–31.

Yamauchi, H., Aminaka, M., Yoshida, K., Sun, G., Pi, J., and Waalkes, M. P. 2004. Evaluation of DNA damage in patients with arsenic poisoning: urinary 8-hydroxydeoxyguanine. *Toxicol. Appl. Pharmacol.* 198:291–296.